A molecular dynamics study of orientational disordering in crystalline sodium nitrate

1989 J. Phys.: Condens. Matter 1 6523

(http://iopscience.iop.org/0953-8984/1/37/002)

J. Phys.: Condens. Matter 1 (1989) 6523–6542. Printed in the UK

A molecular dynamics study of orientational disordering in crystalline sodium nitrate

R M Lynden-Bell†, M Ferrario‡, I R McDonald† and E Salje§

† Department of Chemistry, University Chemical Laboratory, Lensfield Road, Cambridge CB2 1EW, UK

‡ Istituto do Fisica Teorica, Universitá degli Studi di Messina, Casella Postale 50, 98166 S. Agata, Italy

§ Department of Earth Sciences, Downing Street, Cambridge CB2 3EQ, UK

Received 27 October 1988

Abstract. Molecular dynamics computer simulations have been made of the ordered low-temperature and orientationally disordered high-temperature phases of crystalline sodium nitrate. The interionic force model used in the simulations is based on a rigid-ion representation of the electrostatic interactions, supplemented by a set of atom–atom potentials of the Buckingham type. Five simulations have been carried out, covering the temperature range from 293 to 570 K. Where possible, detailed comparison is made with experiment, and generally satisfactory agreement is found. Anion disorder is shown to consist primarily in reorientation about an axis parallel to the crystallographic c direction, but only at the highest temperature studied can the motion be described as that of a free, quasi-two-dimensional rotor.

The spectra of translational and librational lattice modes have been computed and the way in which these change with temperature is discussed in terms of translation–rotation coupling. Numerical estimates are presented of the degree of correlation between translations and rotations at different points in the Brillouin zone, and possible ordering processes are identified. The diffuse scattering predicted by the model is analysed in detail and related to the results of x-ray and neutron scattering experiments. It is suggested that in the high-temperature phase there exist two major ordering processes and that the competition between the two results in the experimentally observed critical exponent for the macroscopic order parameter being significantly less than its classical value. The same argument is formulated on the basis of a Landau-type expression for the free energy. Although the simulations have been limited to the specific case of sodium nitrate, the results should also be helpful in understanding the nature of the corresponding phase transition in calcite.

1. Introduction

Sodium nitrate crystals have the same low-temperature structure as calcite ($R\bar{3}c$). As the temperature is raised from room temperature the anions disorder; they still lie in planes perpendicular to the c axis, but their orientations in these planes becomes disordered. This process culminates in an order–disorder phase transition near 549 K. The transition seems to be continuous and occurs over a remarkably long temperature range. A similar transition occurs at 1250 K in the calcite phase of calcium carbonate, and it is thought that this accounts for the non-linearity of the boundary between the stability fields of the two forms of calcium carbonate, calcite and aragonite, in a pressure–temperature phase diagram. Calcium carbonate is of particular interest to mineralogists since it is an important component of the Earth's crust.

0953-8984/89/376523 + 20 $02.50

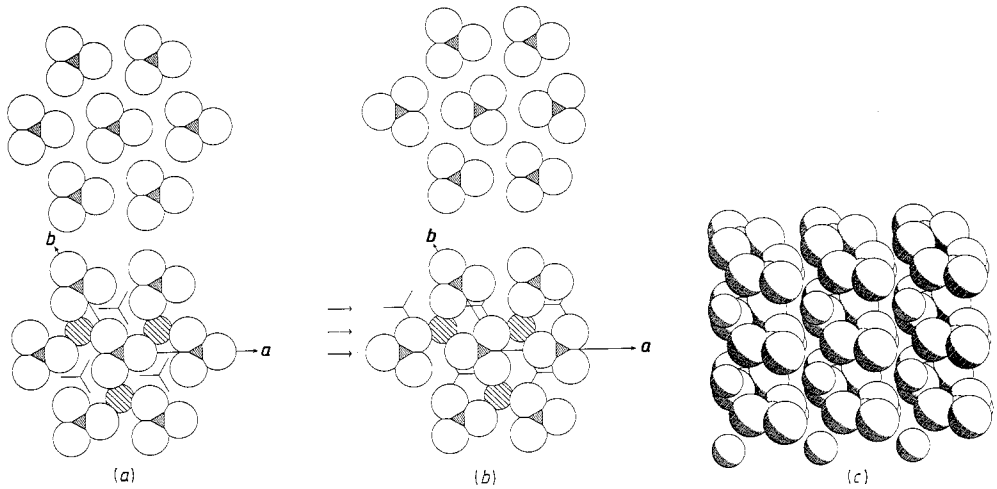

Figure 1. (*a*) Structure of the ordered ($R\bar{3}c$) phase of sodium nitrate. A plane of nitrate ions is shown above, while in the lower figure the cations in the layer below are shaded and the positions and orientations of the nitrate ions in the layer below that are indicated by bond vectors. (*b*) View of the hypothetical F structure. Compared with the $R\bar{3}c$ structure the central row of nitrate ions has been rotated by 180°. The rows indicated by arrows form the F plane and are shifted by 1 Å to the left. (*c*) View of the F structure looking onto the F plane.

The disordering transition in sodium nitrate is used as a model for investigating the disordering in calcite, since it is more readily accessible by experiment than the latter. The onset of disorder is manifest in many properties: the cell parameter c expands anomalously, the Raman-active librational frequency drops and the Raman linewidths of the internal modes increase by a considerably greater extent than is predicted from classical multiphonon scattering. The disordering process has also been studied by birefringence and x-ray diffuse scattering. Recently, Salje and co-workers [1, 2] have used x-ray intensity, excess birefringence, Raman hard-mode linewidth and Raman lineshifts to determine critical exponents from macroscopic order parameters. Although earlier workers suggested that the critical exponent β was equal to 1/2 (Bragg–Williams model) [3] or to 1/3 [4], this most recent work suggests a value of about 0.22 near the transition temperature, rising to the classical value of 1/4 at lower temperatures. Poon and Salje [1] point out that the value of 0.22 is close to that obtained in numerical simulations of the three-state Potts model. Although the nitrate ion has threefold symmetry, it has only two distinct orientations in the low-temperature structure, so that an Ising-like behaviour ($\beta = 0.325$) might have been expected. One can conclude that the disordering mechanism is not straightforward.

None of the experimental methods used thus far gives direct information about the nature of the disordering process on a molecular scale. For example, it is not definitely known whether the orientations of the nitrate ions become random, or whether the two orientations found in the low-temperature structure become equally probable at each site, or whether there are additional favoured orientations in the high-temperature structure. Computer simulation provides a method of answering such questions for well

defined model systems. Although the results pertain to the assumed intermolecular potential, they can be used in the interpretation of observations of real systems, provided the potential is chosen with care.

In an attempt to understand the microscopic behaviour of the system we have carried out molecular dynamics computer simulations of a model for sodium nitrate. We have observed the onset of disorder and many of its macroscopic manifestations. We find that there are competing ordering processes that interfere with each other, which in turn may account for the sharp onset of disorder (β less than the classical value of 1/4) as T_c is approached from below. There is experimental evidence provided by x-ray and neutron diffuse scattering for the existence of these alternative ordering processes in both sodium nitrate and calcite [2].

2. Structure

In the low-temperature structures ($R\bar{3}c$) of sodium nitrate (figure 1(*a*)) there are two orientations for the nitrate anions: one, which we designate by $\sigma = 1$, has one of the N–O bonds lying along the $+\boldsymbol{a}$ direction (in this paper all directions in both real and reciprocal space are referred to hexagonal rather than to rhombohedral axes), while the $\sigma = -1$ orientation has a bond in the $-\boldsymbol{a}$ direction. As the anions have threefold symmetry, these orientations differ by a rotation of 60°. The crystal structure defined by the centres of mass of the ions is $R\bar{3}m$, and does not change at the transition. The average structure of the disordered phase is identical to the centre-of-mass structure, but in the ordered phase, the two nitrate ions in the rhombohedral unit cell have opposite values of σ, so that the unit cell is double that of the disordered structure and the symmetry becomes $R\bar{3}c$. The additional allowed Bragg reflections that arise are due solely to scattering by the oxygen atoms, and occur at the Z point of the reciprocal lattice of the high-temperature structure. This point is also known as the T point [5].

Throughout this paper we shall use coordinates of the reciprocal lattice of the low-temperature $R\bar{3}c$ structure in the hexagonal setting. In these coordinates the Z point of the high-temperature structure is at $\boldsymbol{k} = \boldsymbol{k}_Z = 3\boldsymbol{c}^*$. In this ordering scheme, anions in the same plane perpendicular to $\boldsymbol{c}$ have the same value of σ, while successive planes have alternating values of σ; we shall refer to this as Z ordering. The alternative ordering scheme, which we shall call F ordering, is one in which anions in planes perpendicular to the F direction of the high-temperature lattice have the same value of σ (figures 1(*b*) and 1(*c*)). Because these planes intersect the planes perpendicular to c, F ordering is incompatible with Z ordering and we shall argue that fluctuations in F ordering help to destroy Z ordering in the low-temperature structure thereby lowering the value of T_c. The F ordering shows strong translation–rotation coupling between the orientational variables and the transverse phonon variables; the coupling gives rise to enhanced fluctuations in the anion and cation positions and softens one of the transverse acoustic phonon branches in the ΓF direction. Such coupling is forbidden by symmetry for Z ordering.

In ordering to discuss the ordering processes and the translation–rotation coupling, and to use the simulation results to interpret the x-ray and neutron diffuse scattering observations, it is useful to introduce collective coordinates for both centre-of-mass and orientational displacements. Acoustic phonon, optic phonon and librational variables are defined by

$$
\begin{aligned}
s^{A}_{\alpha}(\boldsymbol{k}) &= N^{-1}\sum_i m_i(r_{i\alpha} - r^0_{i\alpha})\exp(\mathrm{i}\,\boldsymbol{k}\cdot\boldsymbol{r}^0_i) && \alpha = x, y, z \\
s^{O}_{\alpha}(\boldsymbol{k}) &= N^{-1}\sum_i q_i(r_{i\alpha} - r^0_{i\alpha})\exp(\mathrm{i}\,\boldsymbol{k}\cdot\boldsymbol{r}^0_i) && \alpha = x, y, z \\
L_{\alpha}(\boldsymbol{k}) &= N^{-1}\sum_i Z_{iz}Z_{i\alpha}\exp(\mathrm{i}\,\boldsymbol{k}\cdot\boldsymbol{r}^0_i) && \\
& && \alpha = x, y \\
L_z(\boldsymbol{k}) &= N^{-1}\sum_i \sin(3\varphi_i)\exp(\mathrm{i}\,\boldsymbol{k}\cdot\boldsymbol{r}^0_i) &&
\end{aligned}
\tag{1}
$$

where m_i is the mass of the ith ion, $\boldsymbol{r}_i$ its instantaneous centre-of-mass position, $\boldsymbol{r}^0_i$ its equilibrium position and q_i its charge; N is the number of molecules; Z_α is the direction cosine between the crystal α axis ($\alpha = x$, y or z) and the ion-fixed Z axis that is perpendicular to the NO_3^- plane; and φ is the angle between a bond of the ith nitrate ion and the $\boldsymbol{a}$ direction. These coordinates are the acoustic translational, optic translational and out-of-plane and in-plane librational normal modes in the low-$\boldsymbol{k}$ harmonic limit.

It is also useful to introduce a second type of orientational coordinate:

$$Y(\boldsymbol{k}) = N^{-1}\sum_i \cos(3\varphi_i)\exp(\mathrm{i}\,\boldsymbol{k}\cdot\boldsymbol{r}^0_i). \tag{2}$$

Although these coordinates are not independent of the coordinates L_z, they are more useful for the description of the ordering. The ensemble (thermodynamic) averages of the $Y(\boldsymbol{k})$ provide us with set of order parameters. $Q(\boldsymbol{k})$, defined by

$$Q(\boldsymbol{k}) = \langle Y(\boldsymbol{k})\rangle \tag{3}$$

which can readily be measured from the simulation. In the disordered phase all the $Q(\boldsymbol{k})$ are zero, while in the perfectly ordered calcite phase the value of the order parameter at the Z point is unity. In the transition from the disordered structure to the ordered structure, Bragg reflections appear at points in reciprocal space corresponding to this value of $\boldsymbol{k}$. Order parameters with other values of $\boldsymbol{k}$ correspond to alternative hypothetical structures which would have Bragg reflections at these values of $\boldsymbol{k}$. Although all $Q(\boldsymbol{k})$ are zero in the disordered phase, one anticipates that incipient ordering to a structure with a particular $Q(\boldsymbol{k})$ will be manifest in large-amplitude fluctuations in the corresponding coordinate $Y(\boldsymbol{k})$. Such precursor effects should increase as the temperature is lowered towards the critical temperature and can be seen in a simulation.

The possible values of $\boldsymbol{k}$ in the order parameters and the phonon and librational coordinates defined above are restricted to the first Brillouin zone of the centre-of-mass structure ($R\bar{3}m$) (or to an equivalent single unit cell of the reciprocal lattice) because these coordinates are defined with phase factors (exponential terms) involving the equilibrium positions of the centres of mass. Figure 2(*a*) shows the Brillouin zone of the $R\bar{3}m$ structure with the special points Γ, Z, F and L marked. The full $R\bar{3}c$ structure of the low-temperature phase has a reciprocal lattice of the same form, but with the unit cell shrunk by a factor of two in the $\boldsymbol{c}^*$ direction and rotated by 180°. The L point of the centre-of-mass reciprocal lattice becomes the F point of the low-temperature lattice, while the F point of the centre-of-mass lattice lies outside the Brillouin zone of the low-temperature structure and maps onto its F point. In our subsequent discussion of diffuse scattering and of translation–rotation coupling we shall use the $\boldsymbol{k} = (k_a, 0, k_c)$ section through the reciprocal lattice, a plane containing the special points; this is shown in figure 2(*b*). We shall use the notation $\boldsymbol{k}_Z$. $\boldsymbol{k}_F$, etc for the $\boldsymbol{k}$ vectors at the corresponding special points. Character tables for the space groups $R\bar{3}m$ and $R\bar{3}c$ have been constructed by Boyle and Kennedy [5]. There are two irreducible representations for quantities with $\boldsymbol{k}$ in this plane, C_1 and C_2, which are symmetric and antisymmetric, respectively, under

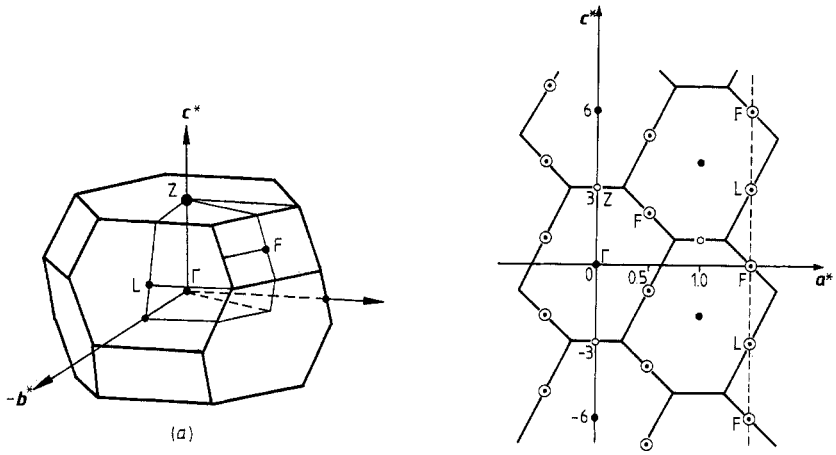

Figure 2. (*a*) Brillouin zone of the R$\bar{3}$m structure defined by the lattice of the centres of mass of the ions. (*b*) Cross section through the reciprocal lattice of the R$\bar{3}c$ structure. The Brillouin zones of the centres-of-mass structure are outlined.

reflections in the plane. One of the transverse phonon coordinates and the orientational coordinate $Y(\boldsymbol{k})$ belong to C_2, while the longitudinal and the other transverse phonon coordinates belong to C_1.

From the simulations we can compute mean-square amplitudes and time correlation functions of the fluctuations in any coordinate. The Fourier transforms of the fluctuations in the phonon and librational coordinates give the corresponding spectra. Fluctuations in the orientational coordinates, $Y(\boldsymbol{k})$, at different $\boldsymbol{k}$ values signal different ordering processes.

3. Potential model and molecular dynamics calculations

3.1. The model

In seeking an interionic potential model to describe the interactions in sodium nitrate, we follow the usual practice of assuming that the total potential energy is a sum of spherically symmetric atom–atom potentials $V_{\alpha\beta}(R)$, where α, β = Na, N or O. The pair potentials are in turn written as the sum of a Coulombic term and a short-range Buckingham potential, i.e.

$$V_{\alpha\beta}(R) = q_\alpha q_\beta / R + A_{\alpha\beta}\exp(-\rho_{\alpha\beta}R) - B_{\alpha\beta}/R^6. \tag{4}$$

The crystal is assumed to be fully ionic. Thus $q_{Na} = e$, where e is the elementary charge, and $3q_O + q_N = -e$. We also suppose that the short-range interaction parameters are related by combining rules of the form

$$A_{\alpha\beta} = (A_{\alpha\alpha}A_{\beta\beta})^{1/2} \qquad \rho_{\alpha\beta} = (\rho_{\alpha\alpha} + \rho_{\beta\beta})^{1/2} \qquad B_{\alpha\beta} = (B_{\alpha\alpha}B_{\beta\beta})^{1/2}. \tag{5}$$

It follows that there are a total of 10 quantities to be specified: nine short-range parameters and one charge. Numerical values for these quantities were derived by a trial-and-error approach based on repeated molecular dynamics simulations, the technical details of which are given below.

As a starting point, the Buckingham potentials used in earlier work on sodium nitrite [6] were adopted, together with the result suggested by *ab initio* calculations [7] for

Table 1. Parameters in the atom–atom potential.

α	q_α (e)	$A_{\alpha\alpha}$ (kJ mol^{-1})	$r_{\alpha\alpha}$ (Å^{-1})	$B_{\alpha\alpha}$ (kJ mol^{-1} Å^6)
Na	1.00	3.1696×10^4	3.155	101
N	0.95	1.408×10^5	3.780	1084
O	−0.65	2.925×10^5	4.180	1085

the isolated ion that $q_0 \simeq -0.6e$. The main criteria used were that the model should adequately reproduce the experimental lattice parameters, including the anomalously large temperature coefficient of expansion along the crystal c axis, while at the same time predicting the onset of orientational disorder of the anions in the correct range of temperature. It was found that at a constant external pressure the calculated lattice parameter a increased, but c decreased as the charge on the oxygen was made more negative, other parameters being held constant. Typically, a increased by between 1% and 2% and c decreased by between 5% and 6% as q_0 was varied between $-0.50e$ and $-0.65e$. These trends led to some simplification of the task of parametrisation. The final values are listed in table 1. They clearly contain a strongly arbitrary element and constitute a representative rather than a definitive model. The short-range repulsions are significantly weaker than in the original work on sodium nitrite. In particular, the parameter A_{00} is 20% smaller than that used earlier. By contrast, in recent calculations for potassium nitrate, Clarke and Smith [8] have combined the original nitrite short-range potentials with a charge model in which $q_0 = -0.77e$, and have been able to reproduce certain of the structural phase transitions of the potassium salt.

3.2. Molecular dynamics calculations

The molecular dynamics calculations were carried out by standard methods. The nitrate ions were treated as fully rigid entities with a N–O bond length of 1.25 Å. The equations of motion were integrated by use of the Verlet algorithm, with a time step of 0.01 ps; the rotation of the nitrate ions was treated by the generalised method of constraints, with the three oxygen atoms chosen as the basic particles in that scheme. Periodic boundary conditions were used and the Coulombic forces and energies were evaluated by the Ewald method; long-range corrections for the truncation of the short-range potentials were calculated in the usual way. Runs were initiated from the fully ordered low-temperature structure, and a substantial period of equilibration was allowed in order that any potential disorder in the system could develop.

Preliminary runs designed to determine a suitable choice of potential parameters were carried out in the constant-temperature, constant-pressure ensemble with the external pressure set to zero; all cell lengths and cell angles were allowed to fluctuate. The system size used in these runs was $3a \times 3b \times 1c$, where the numbers represent the repeat distances along the crystallographic axes of the ordered structure in the hexagonal setting. The basic molecular dynamics cell therefore contained $N = 54$ molecules, i.e. 108 ions or 540 interaction sites. The production runs were made at constant temperature and volume, with values of the lattice parameters taken from experiment. Five such runs were carried out, covering the temperature range from 293 K, where experimentally the crystal is fully ordered, to 570 K, a temperature above that of the experimental order–disorder transition (549 K) but below the melting point (584 K). Four of the runs were made for a system of dimensions $3a \times 3b \times 2c$ ($N = 108$) and one for dimensions $4a \times 4b \times 2c$ ($N = 192$). The run for $N = 192$ was made partly to provide a check on the

results obtained with the smaller system, but more specifically to obtain results at the L and F points in the Brillouin zone which, because of the periodic boundary conditions, are inaccessible for $N = 108$.

Thermodynamics results from the five production runs are shown in table 2. Tabulated quantities include the mean potential energy U and mean electrostatic energy U_c, the diagonal elements of the stress tensor $\mathbf{T}$ and the pressure $P = -\mathrm{Tr}\,\mathbf{T}/3$. The fact that the pressures are of the order of 1 kbar indicates a weak size dependence in the molecular dynamics results, since the potentials used were derived by fitting the experimental lattice constants for a system with $N = 54$. There are also some differences between runs III ($N = 108$) and IIIL ($N = 192$). Overall the results are satisfactory, given the fact that the bulk moduli of ionic compounds are very large, but there is clearly some scope for improvement in the potential.

Contact with experiment can also be made through a comparison of fluctuations in the coordinates of the ionic centres of mass. Such quantities are not experimental observables, but values can be derived from measured neutron or x-ray structure factors if some model of disorder is invoked. The comparison is made in table 3, where the experimental values are those obtained from model I of Lefebvre *et al* [10] as applied to their own scattering measurements. The results are presented in the form of fluctuations in $r_\perp$ and $r_\parallel$, where $r_\perp$ is the displacement of an ion in the *ab* plane and $r_\parallel$ is the displacement along the *c* axis. The agreement between experiment and simulation is as good as could reasonably be expected, giving further support to the choice of potential parameters. In the simulations, however, the displacements seem slightly more isotropic than in the experiments, where fluctuations along the *c* axis are significantly larger than those in the plane.

The degree of orientational disorder was continuously monitored during the molecular dynamics runs. The orientation of the nitrate ions was monitored by observing the single-particle order parameters, η_1 and η_2, defined by

$$\eta_1 = \langle(-1)^L \cos\varphi\rangle \qquad \eta_2 = \langle(-1)^L \cos 3\varphi\rangle.$$

In both these equations L numbers successive layers of nitrate ions which lie perpendicular to the *c* axis and the average is over all nitrates in the molecular dynamics cell. The parameter η_1 is altered by jumps between equivalent positions, so that its value depends on which bond is used to define φ. We used the bond that was initially nearest the ***a*** direction. If the structure is ordered and the motion is purely librational, both these quantities remain close to unity; if rotational motion is dominated by 120° jumps between equivalent positions, η_2 will remain close to unity but η_1 will decay to zero, while if the motion is predominantly between the states $\sigma = +1$ and -1, i.e. 60° jumps, both order parameters will be close to zero. Values of η_1 and η_2 for the production runs are shown in table 2. The phase factor in the definitions of these single-particle order parameters η_2 is such that this parameter is the average value of the collective orientational variable $Y(\boldsymbol{k}_Z)$. Trajectories of values of $Y(\boldsymbol{k}_Z)$ are shown in figure 3. Clearly there is already considerable disorder in run II (450 K), but even at 518 K (runs III and IIIL) disorder is not complete.

4. Selected results and their relation to experiment

4.1. Anion disordering

There are various ways in which the onset and extent of disorder in the simulations can be measured. The primary order parameter $Q(\boldsymbol{k}_Z)$ ($=\langle Y(\boldsymbol{k}_Z)\rangle$) was monitored during

Table 2. Results of molecular dynamics calculations at constant temperature and volume.

Run	N	T (K)	Run length (ps)	a (Å)	c (Å)	U (kJ mol^{-1})	U_c (kJ mol^{-1})	$T_{xx} + T_{yy}$ (kbar)	T_{zz} (kbar)	P (kbar)	η_1	η_2
I	108	293.0	35	5.080	16.844	−729.4	−791.9	0.27	−2.00	0.49	0.96	0.93
II	108	450.0	56	5.090	17.273	−719.5	−780.4	−1.22	−3.72	2.05	0.02	0.47
III	108	518.0	56	5.090	17.468	−715.7	−776.2	−2.15	−4.31	2.87	0.00	−0.20
IIIL	192	518.0	44	5.090	17.468	−713.0	−773.8	−4.13	−2.75	3.67	0.00	0.23
IV	108	570.0	57	5.090	17.750	−712.1	−771.5	−2.01	−3.77	2.60	−0.04	0.02

Statistical uncertainties are typically 0.05 kbar in P and 0.5 kJ mol^{-1} in U.

Table 3. Fluctuations in centre-of-mass coordinates.

			$\Delta r_\perp^2$ (Å^2)		$\Delta r_\parallel^2$ (Å^2)		Δr (Å)	
Run	T(K)	N	Na^+	NO_3^-	Na^+	NO_3^-	Na^+	NO_3^-
I	293	108	0.0194	0.0179	0.0219	0.0172	0.25	0.23
			(0.0184)	(0.0151)	(0.0264)	(0.0236)	(0.25)	(0.23)
II	450	108	0.0476	0.0452	0.0446	0.0354	0.37	0.35
III	518	108	0.0603	0.0573	0.0539	0.0417	0.42	0.40
			(0.0497)	(0.0382)	(0.0548)	(0.0526)	(0.39)	(0.36)
IIIL	518	192	0.0568	0.0536	0.0533	0.0452	0.41	0.39
			(0.0497)	(0.0382)	(0.0548)	(0.0526)	(0.39)	(0.36)
IV	570	108	0.0770	0.0748	0.0634	0.0509	0.46	0.45

Bracketed values are experimental results [10].

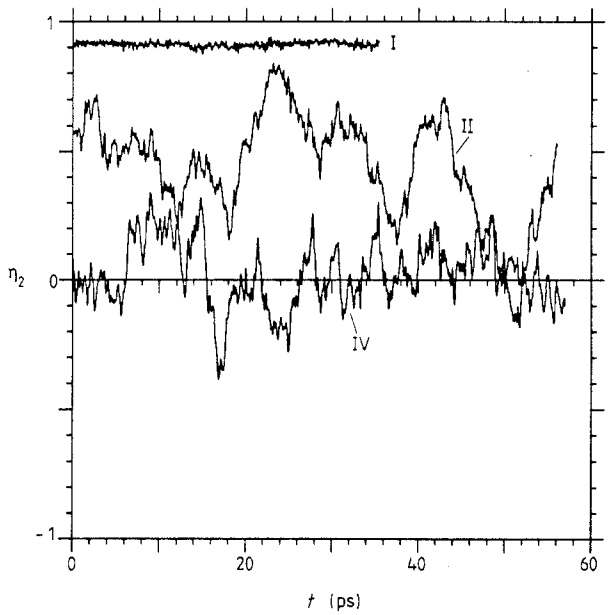

Figure 3. Time evolution of $Y(k_Z)$ for three of the molecular dynamics runs.

each run. The subsequent analysis included the investigation of the probability distribution function for the anion orientation and the dynamics of anion reorientation.

Figure 3 shows the variation of the instantaneous values of $Y(k_Z)$ during trajectories taken from three of the runs. In the low-temperature run, I, there are small fluctuations about an average value near to unity; these are the result of thermal librational motion. Run IV, at 570 K, shows much larger fluctuations about a mean that is near to zero. The runs at intermediate temperatures also show large amplitudes of fluctuation, but with mean values that are not zero on the timescale of the runs (50 ps). The instantaneous value of $Y(k_Z)$ changes sign in runs II and III, which means that in these cases there is a transition from a domain with a positive value of $Q(k_Z)$ to one with a negative value. This raises the interesting point that the order parameter of the system depends on the timescale on which it is measured. These two runs show a non-zero order parameter, with fluctuations about a value that remains steady on timescales of tens of picoseconds, but it seems likely that transitions between the two domains occur faster than the nanosecond timescale. In a macroscopic system the value of Q depends on the spatial

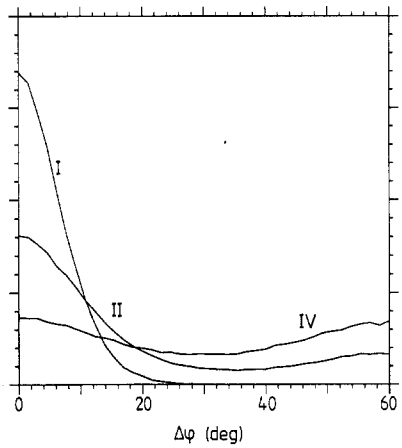

Figure 4. The distribution of angles between nitrate ions and their ideal positions.

extent of the averaging as well as on the timescale of the measurement, so that different experimental techniques may give different values for Q.

In the simulations the anions remain in or close to the plane perpendicular to $\boldsymbol{c}$. The extent to which the molecules tip out of this plane was found to be small even at 570 K (run IV), where in the plane the ions are completely disordered. We also found that there is no preferred direction of tipping relative to the crystal axes. The disorder is shown in the twisting of the anions about the c axis, away from their ideal positions, that is by variations in φ_i. Figure 4 shows the distribution of molecular orientations in the plane plotted as a function of $\Delta\varphi$, the angle between a bond and its ideal position; $\Delta\varphi$ runs between 0° and 60°. In run I the distribution is approximately Gaussian, with a maximum at $\Delta\varphi = 0$, as would be expected for librations in a harmonic potential. As the temperature is increased (runs II and IIIL), a subsidiary maximum appears at 60°, arising from molecules in the 'wrong' orientation. The width of the main peak also increases. In run IV the distribution is symmetrical, but by no means uniform. Although the ions move so that their orientations are randomised, they still experience a crystal field favouring two orientations, and cannot be said to be rotating freely. There is no evidence of preferred orientation in the 'aragonite' direction at 30°, as proposed by Strømme [11], and the results agree with neutron scattering results [10].

The dynamics of anion reorientation is strongly affected by correlated motion of neighbouring ions. This can be seen both in the non-exponential decay of single-ion time correlation functions and in the different rates of decay of collective orientational variables for different values of $\boldsymbol{k}$. The time correlation function of the single-ion order parameter σ, defined to be $+1$ or -1 according to the sign of $\cos 3\varphi_i$, was computed. This order parameter was used because it is unaffected by librational motion, but it changes if an ion moves between the two favoured orientations. Its time correlation function was found to decay non-exponentially, at least for the greater part of the total decay. The reorientation process cannot, therefore, be described by a first-order rate equation or by a lifetime for a particular orientation. Some idea of the relative rates of decay can, however, be gained by comparing the time taken for the correlation function to decay to e^{-1} of its original value (τ in table 4). In all runs except I (totally ordered), the fluctuations near the F and L points decay much more slowly than those near the Γ point. This is because the system is close to the critical temperatures associated with Z and F ordering. But one can also (and equivalently) describe the variation of behaviour with $\boldsymbol{k}$ in terms of correlations in real space: in this case, by the existence of correlated

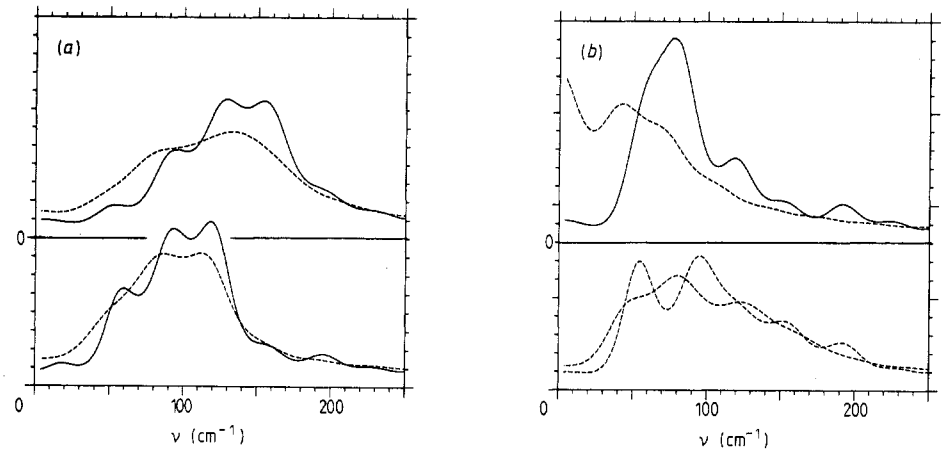

Figure 5. (*a*) Fourier transforms of the autocorrelation functions of the x components of ion velocity (below) and angular velocity (above). The full curves are for run I (350 K) and the broken curves are for run III (518 K). The non-zero baseline is an artefact of the maximum entropy method used for Fourier transformation. (*b*) As (*a*), but for the z components of ion velocity and angular velocity.

Table 4. Time taken for the correlation function to decay to e^{-1} of its original value.

Run	I	II	III	IIIL	IV
τ (ps)	—	4.2	0.8	0.8	0.4

dynamics of neighbouring ions. Further circumstantial evidence for correlated motion is found when trajectories of the orientations of neighbouring ions are compared.

4.2. Spectra of lattice modes

The spectra of translational and librational lattice modes were found by taking the Fourier transforms of the time correlation functions of the phonon coordinates defined in equation (1). Phonon spectra can be measured experimentally for all values of $\boldsymbol{k}$ by inelastic neutron scattering [10] and in the $\boldsymbol{k} \rightarrow 0$ limit by infrared and Raman spectroscopy [12–14]. It is generally found that, while reasonable agreement can be found between the acoustic frequencies found in rigid-ion simulations and in experiment, the omission of polarisability from the model leads to discrepancies between the optic frequencies. Table 5 shows the assignment and symmetries of the zone centre modes in the $R\bar{3}c$ and $R\bar{3}m$ structures together with the frequencies found in the simulations and in the experiments. The interpretation of the spectra of the low-temperature phase is straightforward, but the selection rules in the high-temperature phase pose a problem. The space group $R\bar{3}m$ applies only to the average, not to the instantaneous structure. The criterion as to whether the average structure or the instantaneous structure is the one relevant to a spectroscopic measurement is whether the ratio of the timescale of structural changes to the inverse of the frequency shift between the spectra of each structure is less than or greater than unity. In a frozen disordered structure (where this ratio would be very large), one would expect the selection rules to break down and the observed spectra to be broad superpositions, i.e. to be inhomogeneously broadened. If the ratio were less than one, the nitrate ions would be rotating fast enough to appear disc-like, and the selection rules of the $R\bar{3}m$ structure would apply strictly. Experimentally the

Table 5. Frequencies and assignment of zone centre bands.

Assignment	T_z^{0p}		R_z	$T_z(Na^+)$	$T_z(NO_3^-)$	R_z	T_x^{0p}, T_y^{0p}	R_x, R_y	$T_x, T_y(Na^+)$	$T_x, T_y(NO_3^-)$	R_x, R_y
Symmetry ($R\bar{3}c$)	Γ_2^-		Γ_2^+	Γ_1^-	Γ_2^+	Γ_2^-	Γ_3^-	Γ_3^+	Γ_3^-	Γ_3^+	Γ_3^-
Symmetry ($R\bar{3}m$)	Γ_2^-		Γ_2^+	T_2^-	T_1^+	T_1^-	Γ_3^-	Γ_3^+	T_3^-	T_3^+	T_3^-
Activity	IR		Silent	Silent	Silent	IR ($<T_c$)	IR	Raman	IR ($<T_c$)	Raman ($<T_c$)	IR ($<T_c$)
	TO	LO									
v (cm^{-1}) Run I	183	280	125	205	163	89	195	160	182	95	95/100
Experiment	214	262				90	209	191	175	100	87

Experimental frequencies are from [12] (infrared) and [13] (Raman).

infrared and Raman transitions broaden, but do not disappear as the phase transition is traversed. This suggests that the timescale for nitrate reorientation is slow compared with the spectroscopic timescale. In the simulations the timescale for reorientation is ~10 ps in run III and ~3 ps in run IV. The corresponding frequencies are 0.016 THz (0.53 cm^{-1}) and 0.053 THz (1.8 cm^{-1}) respectively. These timescales make it plausible that the selection rules of the average structure are not those appropriate to the infrared and Raman measurements.

Linewidths in the simulation are found to increase with $\boldsymbol{k}$ for both the acoustic and librational modes. The longitudinal optic modes are broadest at small $\boldsymbol{k}$ and have shapes similar to the one-phonon density of states, suggesting that the anharmonicity of the system allows transitions to combinations of optic and acoustic modes. Mixing of modes of different types, but the same symmetry, is common and shows, for example, in the appearance of the same bands in spectra obtained from the correlation functions of both librational and translational coordinates. For $\boldsymbol{k}$ values in directions of low symmetry, mixing leads to complex spectra with many peaks.

In the runs at higher temperatures the phonon spectra are considerably broader, and the optic phonons in the simulation disappear beneath the noise. Experimentally the Raman modes soften as well as broaden as the temperature is raised [12]. This is also found in the simulations and is principally due to the expansion of the c axis, which allows the ions to move further apart. There is also a softening of the transverse acoustic branch and both librational branches in the $\boldsymbol{c}^*$ direction. Translation–rotation coupling between the orientations and displacements of the ions occur in the partially ordered and disordered phases. We find that this reaches a maximum at the F point. One result is the appearance of a central relaxational component in the phonon spectra of translational modes of appropriate symmetry. As this coupling is important for the discussion of the x-ray diffuse scattering and, we believe, affects the disordering process, we leave the detailed discussion to the next section.

4.3. Hard-mode Raman spectra

Experimental observations of the internal modes have also been made [13, 15]. The lines broaden more than expected as the temperature is raised towards that of the phase transition. This behaviour may in part be due to fluctuations in the local environment, but there is also a contribution due to anharmonicity, which allows transitions to combinations of internal modes and phonon modes. If there is little dispersion of the internal modes, the resulting lineshape should be the same as the one-phonon density of states, which in turn is proportional to the Fourier transform of the ion centre-of-mass velocity autocorrelation function. The latter can be calculated directly from the simulation. Figure 5 shows the Fourier transforms of the x and z components of both linear and angular velocities. The sum of the x, y and z angular velocity autocorrelation functions is identical to the one-libron density of states in the harmonic approximation. The most dramatic change on going from run I (ordered, full curve) to run III (partially ordered, broken curve) is the appearance of a non-zero intercept in the z angular velocity spectrum. This is the result of the reorientation of the nitrate ions. There is also a shift of the maxima to lower frequencies, especially for the T_z phonons.

5. Nature of the ordering transition

5.1. Order parameters

As described in § 2, the ensemble (thermodynamic) averages of the orientational coordinates $Y(\boldsymbol{k})$ provide us with a set of order parameters, $Q(\boldsymbol{k})$, which can readily be

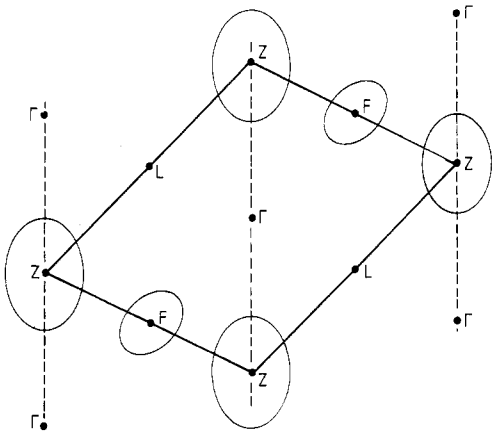

Figure 6. Regions of large fluctuations in the orientational coordinates $Y(k)$ in the disordered phase are shown by ellipses on a cross section of the reciprocal lattice containing the special points. The first Brillouin zone of the R3m structure is shown.

measured from the simulation. In the disordered phase incipient ordering to a structure with a particular $Q(k)$ will be manifest in large-amplitude fluctuations in the corresponding coordinate, $Y(k)$. Such precursor effects should increase as the temperature is lowered towards the critical temperature.

5.2. *Observed fluctuations in Y(k)*

In run IV, which is completely disordered, fluctuations in $Y(k)$ are larger than average in two regions of reciprocal space, namely along c^*, rising to a maximum at the zone boundary point Z ($3c^*$ in the hexagonal setting of the low-temperature R$\bar{3}c$ structure), and along the lines from Γ to the three equivalent F points. The fluctuations along the lines from Γ to the L points are less than average. As the temperature is reduced to the conditions of run III (which is partially ordered), the mean-square values of $Y(k)$ are reduced in most parts of reciprocal space by about 10%, but at the Z point ($3c^*$) and at points along c^* nearby ($2.5c^*$ and $2c^*$) they are considerably enhanced, and they are slightly enhanced at the two accessible points nearest the Γ–F direction. The F point itself is inaccessible in this simulation; a larger simulation at the same temperature (run IIIL) showed a local maximum at that point. These results are shown schematically in figure 6. The two regions of enhanced fluctuations in $Y(k)$ correspond to the two ordering processes mentioned in the introduction. They both contribute to x-ray and neutron diffuse scattering, as we discuss later.

The onset of order in rotator phases is often accompanied by a distortion of the lattice, due to a simultaneous freezing-in of a phonon mode with the onset of a non-zero average for the order parameter Q, so that the transition is of mixed displacive and order–disorder type. While it is not necessary for an orientational ordering transition to be accompanied by such a distortion, and indeed the Z-ordering process does not do so (for symmetry reasons), if distortion and orientational ordering occur simultaneously they provide another way in which incipient ordering can be studied in simulations [16]. The phenomenon is known as translation–rotation coupling and results from coupling terms in the free energy between a phonon displacement coordinate and an orientational coordinate at the same k value [17]. The consequences of this coupling are that fluctuations in the phonon and orientational coordinates in the disordered phase are correlated with correlation coefficient Ξ, fluctuations in both coordinates are enhanced by a factor of $(1 - \Xi^2)^{-1}$, and that T_c is raised as the phonon displacement assists the ordering. Phonon dynamics are also affected by the coupling.

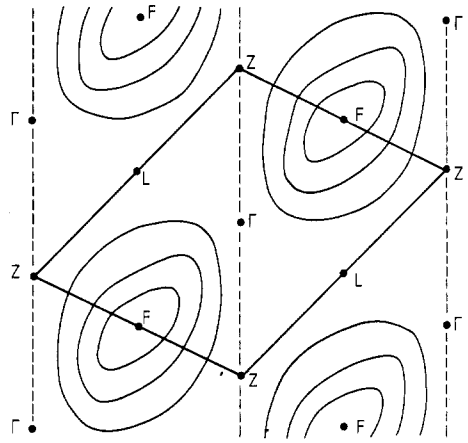

Figure 7. The extent of translation–rotation coupling in runs III and IIIL is shown for k vectors in a cross section of the reciprocal lattice. Contours of Ξ^2 are drawn at intervals of 0.25; $\Xi^2 = 0$ on the broken line, 0.23 at the L points and 0.93 at the F points.

Translation–rotation coupling may only occur between $s(\boldsymbol{k})$ and $Y(\boldsymbol{k})$ variables of the same symmetry. In the space group $R\bar{3}m$ mixing between $Y(\boldsymbol{k})$ and phonons is forbidden by symmetry at the Γ point and for $\boldsymbol{k}$ values along $\boldsymbol{c}^*$. Hence there is no lattice distortion and no translation–rotation coupling associated with the Z ordering. When the wavevector lies in one of the planes containing Γ, Z and one of the three equivalent pairs of F and L points (see figure 2(*b*)), $Y(\boldsymbol{k})$ may couple to the transverse phonon whose displacement is perpendicular to the plane. We measured the extent of this coupling through the correlation coefficient, Ξ, defined by

$$\Xi(\boldsymbol{k}) = \langle s(\boldsymbol{k})^* Y(\boldsymbol{k})\rangle / (\langle s(\boldsymbol{k})^* s(\boldsymbol{k})\rangle \langle Y(\boldsymbol{k})^* Y(\boldsymbol{k})\rangle)^{1/2}. \tag{6}$$

The value of Ξ^2 varies between zero where there is no correlation to one for complete correlation [17]. The latter occurs only at the transition point to a new phase in which both coordinates are non-zero on average. The angular brackets in this expression for Ξ denote ensemble averages, which may readily be computed from the simulation. Figure 7 shows contour plots of the values of Ξ^2 found in the simulation for $\boldsymbol{k}$ vectors in the ΓZF plane shown in figure 2(*b*). The high value of Ξ^2 (0.93) found at the F point indicates that fluctuations at the F point are nearly large enough to cause a phase transition to the F-ordered phase which would be monoclinic (figures 1(*b*) and (*c*)). We conclude that F ordering is a serious competitor to Z ordering, at least in this model. Rotation–translation coupling is forbidden by symmetry along the $\boldsymbol{c}^*$ axis, so this method of probing ordering in the simulation cannot be used for Z ordering.

5.3. X-ray diffuse scattering and neutron inelastic scattering

There is some evidence in the x-ray diffuse scattering experiments for the existence of fluctuations in both Z and F ordering, although it is difficult to distinguish between scattering due to phonon fluctuations and orientational fluctuations near the F point. Early x-ray observations of the disordered phase [18] showed three types of x-ray diffuse scattering: pancakes around the Bragg points, bridges between Bragg points, and scattering around the superlattice points. Referred to a single unit cell of the reciprocal lattice, the pancakes are around the Γ points perpendicular to the $\boldsymbol{c}^*$ axis, the bridges are along the Γ–F directions with maxima at the F points, and the superlattice scattering is near the Z points. All the diffuse scattering is very weak.

The simulation data show the effects described above in both x-ray and neutron diffuse scattering. The intermediate scattering function. $F(\boldsymbol{q}, t)$ and the diffuse scattering, $S(\boldsymbol{q})$, at a point $\boldsymbol{q}$ in reciprocal space are calculated from the fluctuations in $\rho(\boldsymbol{q})$,

$$\rho(\boldsymbol{q}) = N^{-1} \sum_i b_i \exp(-\mathrm{i}\boldsymbol{q} \cdot \boldsymbol{r}_i), \tag{7}$$

by

$$S(\boldsymbol{q}) = \langle \rho(\boldsymbol{q})\rho(\boldsymbol{q}^*)\rangle \qquad F(\boldsymbol{q}, t) = \langle \rho(\boldsymbol{q}, 0)\rho(\boldsymbol{q}^*, t)\rangle \tag{8}$$

and $S(\boldsymbol{q}, \omega)$ is the time Fourier transform of $F(\boldsymbol{q}, t)$. In equation (7) b_i is the scattering length for the ith atom. The neutron scattering lengths are Na = 0.36, N = 0.94 and O = 0.58. The equivalent factors for x-ray scattering are the form factors, which are dependent on $\boldsymbol{q}$. These were calculated using standard formulae [19]. In addition, scattering was calculated using the hypothetical scattering lengths Na = 0.0, N = 1.0 and O = −3.0, which were chosen to eliminate the effects of centre-of-mass motions from the scattering. The results of these calculations will be called orientational scattering.

Diffuse scattering at a point $\boldsymbol{q}$ in reciprocal space must be related to fluctuations in either phonon coordinates or librational coordinates or the orientational coordinate $Y(\boldsymbol{k})$ at the vector $\boldsymbol{k}$ in the first Brillouin zone which corresponds to $\boldsymbol{q}$. By comparing the amplitudes of these fluctuations with the computed values of $S(\boldsymbol{q})$, we were able to identify the superlattice scattering with fluctuations in Z ordering and the pancakes with large transverse acoustic phonon fluctuations for small $\boldsymbol{k}$ values and displacements in the c direction. The latter observation suggests that the model has a low value of the corresponding elastic constant C_{44}, which is also abnormally low in the real crystal [20, 21]. The bridges are associated both with the F-ordering fluctuations and with transverse phonon displacements. Even in the completely ordered structure, neutron measurements [22] show that one of the transverse phonon modes is softened as the F point is reached. This softening, by itself, would give rise to some x-ray diffuse scattering. As the disorder increases, fluctuations in these phonons are enhanced by translation–rotation coupling, and, in addition, scattering will occur from fluctuations in the orientational variable.

The character table of the space group $R\bar{3}m$ shows four symmetry species (irreducible representations), namely F_1^+, F_2^+, F_1^- and F_2^-, associated with the F point. In order to observe contributions from the F ordering and the transverse phonons with the same symmetry (F_1^-) that are softened by translation–rotation coupling, it is necessary to have a component of $\boldsymbol{q}$ which is perpendicular to the plane containing $\boldsymbol{k}_F$ and $\boldsymbol{c}^*$: we shall call such a $\boldsymbol{q}$ an out-of-plane $\boldsymbol{q}$. In-plane $\boldsymbol{q}$s, which lie in this plane, only show F_2^- phonons, that is phonons with displacements in the plane. This contrast is illustrated in figure 8 which shows the magnitude of the diffuse scattering for x-rays and neutrons as reciprocal space is traversed along a line parallel to $\boldsymbol{c}^*$ passing through F and L points. One such line is marked in figure 2(b). The in-plane $\boldsymbol{q}$s, $(0, 1.5, \zeta)$, show no enhanced scattering at the F points; the small maxima seen are associated with the edges of the pancakes around Γ points. The out-of-plane $\boldsymbol{q}$s, $(-3, 1.5, \zeta)$, show enhanced scattering at the F points, and nothing at the L points. This effect is most marked for the hypothetical orientational scattering (the curve with no symbols). The computed neutron and x-ray scattering results show cancellation at F points in alternate zones. This shows that a large contribution to the diffuse scattering comes from acoustic (as opposed to optic) phonons.

The contrast between the in-plane and out-of-plane $\boldsymbol{q}$ scattering also shows up in the dynamics. Figures 9 and 10 show $F(\boldsymbol{q}, t)$ and $S(\boldsymbol{q}, \omega)$ computed from the simulation for neutron scattering for the two F points at $\zeta = 0$ in figure 8. The large fluctuations seen in the scattering at the out-of-plane $\boldsymbol{q}$ decay more slowly than those seen at the in-plane $\boldsymbol{q}$, giving a sharp central peak in the neutron spectrum.

5.4. Interpretation of ordering in $NaNO_3$

Landau theory often provides a useful method for describing ordering in orientationally disordered crystals. The free energy of such a system is written as a Landau expansion in terms of powers of orientational order parameters $Q(\boldsymbol{k})$:

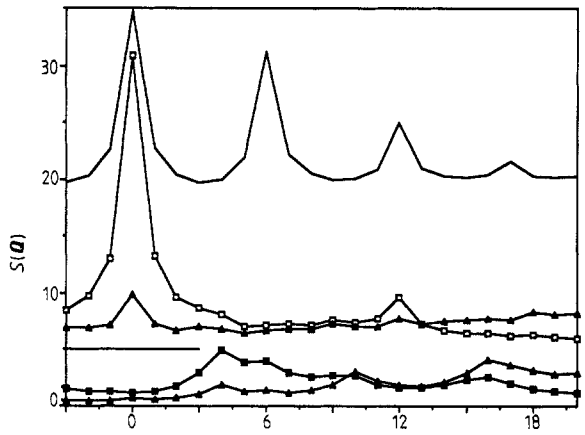

Figure 8. Calculated diffuse scattering for in-plane wavevectors $q = (0, 1.5, \zeta)$ (below) and out-of-plane wavevectors $q = (\bar{3}, 1.5, \zeta)$ (middle). X-ray scattering is shown by square symbols and neutron scattering by triangular symbols. The top curve is the orientational scattering which shows maxima at every F point.

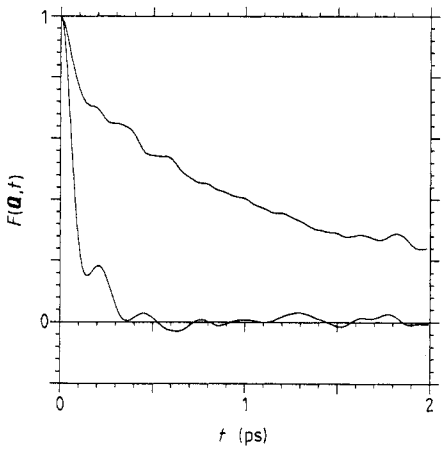

Figure 9. The time dependence of $F(\boldsymbol{q}, t)$ for neutron scattering for a $\boldsymbol{q}$ vector $(= (0, 1.5, 0))$ at an F point in the b^*c^* plane of the reciprocal lattice (below), and for a $\boldsymbol{q}$ vector $(= (-3, 1.5, 0))$ with a component perpendicular to this plane (above). The out-of-plane scattering decays more slowly.

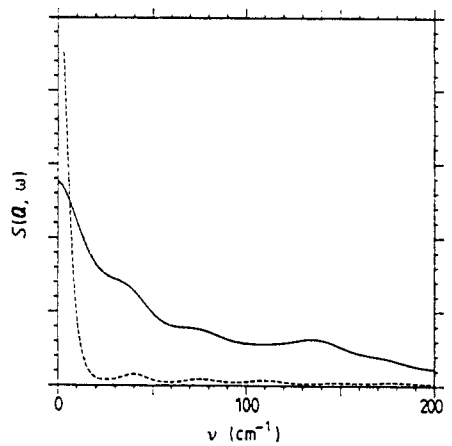

Figure 10. $S(q, \omega)$ for neutron scattering at the two $\boldsymbol{q}$ vectors of figure 9 (full curve: $(0, 1.5, 0)$; broken curve: $(-3, 1.5, 0)$).

$$G = G_0 + \sum A_i Q(\boldsymbol{k}_i)^2 + \sum C_{ij} Q(\boldsymbol{k}_i)^2 Q(\boldsymbol{k}_j)^2 + \sum D_{ij} Q(\boldsymbol{k}_i)^2 Q(\boldsymbol{k}_j)^4. \tag{9}$$

Every term in this expression must be completely symmetrical under the operations of the space group of the disordered phase. The equilibrium configuration is found by minimising this expression with respect to all the order parameters. If all the coeficients, A_i, are positive, there is no net order, i.e. $Q(\boldsymbol{k}_i) = \langle Y(\boldsymbol{k}_i) \rangle = 0$, and the symmetry is not broken. Fluctuations in the order parameters are described by

$$\langle Y(\boldsymbol{k}_i)^2 \rangle = kT/A_i \qquad T > T_c. \tag{10}$$

In Landau theory, at least one of the coefficients has the form $A_i = a_i(T - T_c)$, so as T_c

is approached from above the amplitude of the fluctuations increases rapidly; their dynamics also slow down. Below T_c the order parameter $Q(\boldsymbol{k}_i)$ is no longer equal to zero and the symmetry is broken. The theory predicts that, as the temperature is lowered further, either the mean value of the order parameter increases with critical exponent $\beta = 1/2$, and that the fluctuations about this value decrease as $(T_c - T)^{-1}$, or, if, as often happens in practice, the coefficients of the quartic terms (C_{ij}) are small, $\beta = 1/4$ and the mean-square fluctuations decrease as $(T_c - T)^{-1/2}$. This latter behaviour is often known as tricritical, as it is found near a tricritical point. In the simulation we have identified two potential ordering processes, and the corresponding order parameters $Q(\boldsymbol{k}_Z)$ and $Q(\boldsymbol{k}_F)$ must be included in the Landau free-energy expression. The Z point is unique, but there are three symmetry-related F points so that each $Q(\boldsymbol{k}_F)$ is threefold degenerate, $Q(\boldsymbol{k}_F) = (f_1, f_2, f_3)$, and the terms in the Landau expression arising from $Q(k_F)$ are

$$G_F = G_0 + A_F(f_1^2 + f_2^2 + f_3^2) + C_{1F}(f_1^4 + f_2^4 + f_3^4) + C_{2F}(f_2^2 f_3^2 + f_3^2 f_1^2 + f_1^2 f_2^2).$$

The formula for the Landau free energy of sodium nitrate is the sum of this expression together with contributions from $Q(k_Z)$ and all cross terms that are totally symmetric, such as

$$Q(k_Z)^2(f_1^2 + f_2^2 + f_3^2).$$

It has been found that such terms may arise from the coupling of the orientational order parameters with the strain [23], for example; in this case terms such as $Q(k_Z)^2\varepsilon$ and $f_1^2\varepsilon$ may occur. The anomalously large coefficient of expansion along the c axis below T_c in both calcite and sodium nitrate suggests that these terms should be included.

From experimental observation we know that the primary order parameter is $Q(\boldsymbol{k}_Z)$ and that the contribution of the fourth-order term is small ($C \simeq 0$), since the value of the critical exponent β is $1/4$ rather than $1/2$ at temperatures well below T_c. However, the presence of significant flucuations in other order parameters may have a large influence on the ordering and on the phase transition.

Landau theory is only approximate. It is based on some form of a mean-field approximation and is known to fail in the Ginzburg interval, which is the temperature range in the immediate vicinity of T_c where the critical fluctuations are larger than the order parameter. It has been shown both experimentally and theoretically that the Ginzburg interval is often very small (or absent) for ferro-elastic systems [24]. Taking the large spontaneous strain (shown by the large temperature coefficient of the lattice constant c) of $CaCO_3$ and $NaNO_3$ as evidence for a high contribution of elastic energy to the total excess Gibbs free energy, one might expect to find classical Landau behaviour to remain valid very close to T_c. Indeed, tricritical Landau behaviour ($Q \propto (T_c - T)^{-1/4}$) is found for temperatures between room temperature and T_c for calcite [25]. Sodium nitrate by contrast shows a non-classical exponent, $\beta = 0.22$, over a large temperature range (between $T \simeq 460$ K and T_c). Tricritical Landau behaviour occurs at lower temperatures (between 50 and 460 K). The question arises, therefore, whether the non-classical behaviour is due to large fluctuations of the order parameter, due to order parameter coupling, due to cross-over to a different transition mechanism as the critical temperature is approached from below, or due to some other effect.

A clear distinction between these different suggestions appears very difficult on purely experimental grounds [1]. On the basis of our molecular dynamics simulations, however, we suggest that coupling between the F and Z order parameters plays a crucial role. This coupling arises both from the direct interaction between the corresponding coordinates, or indirectly via coupling of both to the elastic strain. The direct interaction is due to interference between the order parameters, which arises because any given

nitrate position cannot be more than totally ordered. If the lattice is, say, in the perfectly ordered Z structure, then there can be no fluctuations in any other order parameter. Large fluctuations of the F order parameter help to destroy the Z structure and therefore reduce T_c. This interference can most easily be seen by transforming back from reciprocal space to real space. At some position i the instantaneous value of the orientational coordinate of molecule i, $\cos 3\varphi$, is given by a sum of the collective variables at every wavevector:

$$\cos(3\varphi_i) = \sum_{k} \exp(-i\boldsymbol{k} \cdot \boldsymbol{r}_i^0)\, Y(\boldsymbol{k}).$$

As the modulus of $\cos 3\varphi$ cannot exceed unity at any site, at any instant the fluctuations in the coordinates corresponding to order parameters are restricted by the condition

$$\sum_{k} |Y(\boldsymbol{k})| < 1$$

which means that instantaneous fluctuations in one orientational coordinate help to destroy order in another coordinate. In this case there are large-amplitude fluctuations in $Y(\boldsymbol{k}_F)$ near T_c, and these help to destroy the $Q(\boldsymbol{k}_Z)$ order, lowering T_c.

In the Landau expresion this effect has two consequences: firstly, it contributes a positive biquadratic coupling between $Q(\boldsymbol{k}_F)$ and $Q(\boldsymbol{k}_Z)$, and secondly, even when the order parameter $Q(\boldsymbol{k}_F)$ is zero it gives a renormalisation of the coefficient of $Q(\boldsymbol{k}_Z)^2$ which becomes

$$A_Z(\text{eff}) = (A_Z + \lambda\langle Y(\boldsymbol{k}_F)^2\rangle)$$

where λ is a positive constant, resulting in a lowering of T_c. The temperature dependence of $A_Z(\text{eff})$ is affected by the change in amplitude of the fluctuations in $Y(k_F)$ so that the critical exponent β is reduced from its classical value; this may account for the lowering of β from the classical value of 0.25 to the observed value of 0.22.

Biquadratic coupling between $Q(\boldsymbol{k}_F)$ and $Q(\boldsymbol{k}_Z)$ in the Landau expression also arises indirectly if both order parameters couple to the strain. Salje and Devarajen [23] have investigated the general properties of Landau systems with strain-induced coupling between two order parameters. They show that the effective biquadratic coupling is positive if the coupling of the two order parameters to the strain has opposite signs. They find a wealth of possible phase diagrams depending on the values of the parameters in the Landau expression. In particular, even where the ground state corresponds to one of the order parameters ($Q(\boldsymbol{k}_Z)$ in our case), one can get changes to mixed phases and/or to other ordered phases before reaching the completely disordered phase.

5.5. Molecular aspects of the ordered structures

Figure 1(*a*) shows the calcite structure with Z ordering. The structure is held together primarily by the attraction between cations and oxygen atoms in the layers above and below. Within a nitrate layer repulsion between the oxygen atoms causes the nitrates to remain apart and the near octahedral arrangement of oxygens around each sodium ensures a minimum repulsion between oxygens in one layer and the next layer above. Figure 1(*b*) shows the hypothetical F-ordered structure viewed from above. Again, each sodium ion interacts with three oxygen atoms in the layer above and below in much the same way as in the Z structure. The relation of the oxygen atoms in these two layers is, however, less favourable, so one might expect the c parameter to be larger in the F structure. In the disordered structure this interlayer repulsion is likely to be intermediate between these two, and is certainly greater than in the Z structure. This explains the

large thermal expansion along the c axis and the coupling between the Z order parameter and the strain. One can also see the reason for the large rotation–translation coupling in the F structure. In figure 1(b) alternate F planes have had to be translated relative to each other in order to pack the nitrate ions in their layers after rotating alternate rows of ions from the $\sigma = +1$ to the $\sigma = -1$ orientations.

Acknowledgments

We thank W Poon, W W Schmahl and M T Dove for discussions and for communicating experimental results before publication, and the Leverhulme Trust for financial support (to ES).

References

[1] Poon W C-K and Salje E 1988 *J. Phys. C: Solid State Phys.* **21** 715
[2] Schmahl W W and Salje E 1989 *Phys. Chem. Minerals* submitted
[3] Shen T Y, Mitra S S, Casella R C and Trevion S F 1975 *Phys. Rev.* B **12** 4530
[4] Klement W 1970 *J. Phys. Chem.* **74** 2753
[5] Boyle L L and Kennedy J M 1988 *Z. Kristallogr.* **182** 39
[6] Klein M L and McDonald I R 1982 *Proc. R. Soc.* A **382** 471
[7] Wyatt J F, Hillier I H, Saunders V R, Connor J A and Barber M 1971 *J. Chem. Phys.* **54** 5311
[8] Clarke J H R and Smith W 1989 *J. Phys.: Condens. Matter* **1** at press
[9] Allen M P and Tildesley D J 1987 *Computer Simulation of Liquids* (Oxford: OUP)
[10] Lefebvre J, Fouret R and Zeyen C M E 1984 *J. Physique* **45** 1317
[11] Strømme K O 1969 *Acta Chem. Scand.* **23** 1616; 1972 *Acta Chem. Scand.* **26** 477
[12] Brehat F and Wyncke B 1985 *J. Phys. C: Solid State Phys.* **18** 4247
[13] James D W and Leong W H 1968 *J. Chem. Phys.* **49** 5089
[14] Neumann G and Vogt H 1978 *Phys. Status Solidi* b **85** 179
[15] Poon W C-K and Salje E 1988 private communication
[16] Lynden-Bell R M, McDonald I R and Klein M L 1983 *Mol. Phys.* **57** 865
[17] Michel K H and Naudts J 1977 *J. Chem. Phys.* **67** 547; 1978 *J. Chem. Phys.* **68** 216
[18] Shinnaka Y 1964 *J. Phys. Soc. Japan* **19** 1281
[19] Cromer D T and Waber J T 1974 *International Tables of Crystallography* vol IV, ed. J A Ibers, W C Hamilton and G D Reick (Birmingham: Kynoch)
[20] Hearmon R F S 1971 *Phys. Status Solidi* a **5** K183
[21] Ramachandran V, Ibrahim M M, Padaki V C and Gopal E S R 1981 *Phys. Status Solidi* a **67** K49
[22] Schmahl W W private communication
[23] Salje E and Devarajan V 1986 *Phase Transitions* **6** 235
[24] Bismayer U, Salje E, Glazer A M and Cosier J 1986 *Phase Transitions* **6** 129
Salje E 1985 *Phys. Chem. Minerals* **12** 93; 1987 *Phys. Chem. Minerals* **14** 181
[25] Dove M T and Powell B M 1989 *Phys. Chem. Minerals* **16** 503